

Soft Nanotube Hydrogels Functioning As Artificial Chaperones

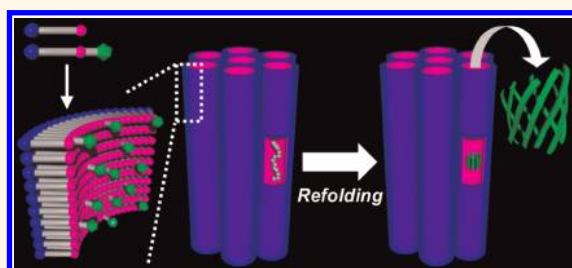
Naohiro Kameta,* Mitsutoshi Masuda, and Toshimi Shimizu

Nanotube Research Center (NTRC), National Institute of Advanced Industrial Science and Technology (AIST), Tsukuba Central 5, 1-1-1 Higashi, Tsukuba, Ibaraki 305-8565, Japan

Nanobiotechnology regarding the refolding of proteins has attracted much attention in the biological and medical fields, because it can be useful to understand proteomics and diseases caused by the misfolding of proteins. Refolding control is also very important for simple, low-cost, and large-scale production of proteins. However, protein production that depends on the broad use of *Escherichia coli* has some problems, including aggregation of partially folded intermediates and the formation of insoluble and inactive inclusion bodies. To prevent these problems, various agents, such as amino acids, carbohydrates, polyethyleneglycols (PEGs), detergents, and cyclodextrins (CDs), have been used as additives.^{1,2} Furthermore, nanomaterial science based on supramolecular self-assembly systems has enabled the construction of micelles,^{3–6} liposomes,^{7–11} block polymers,^{12,13} and nanoparticles^{14–20} that can act as additive agents and assist the refolding. Polysaccharides^{21–25} and CD-functionalized polymers^{26–29} have also been used and can effectively remove detergents from complexes formed between proteins and detergents. However, controlling an adequate interaction between the additive agents and the proteins, optimizing the refolding conditions, and removing the additive agents after the refolding process remain problematic. Consequently, these systems offer low yields and are applicable to a limited range of proteins.

In living systems, molecular chaperones such as GroEL-GroES assist in the refolding process.^{30,31} They possess a nanospace that selectively traps unfolded nascent proteins or refolding intermediates without causing irreversible aggregation.^{32–35} Recently, artificial molecular chaperones based on mesoporous inorganic materials, such as zeolites,^{36–42} and nanospace-polymer materials,⁴³ such as nanogels, have been reported. Zeolites and nanogels self-assembled from polysaccharides modified with hydrophobic side chains were

ABSTRACT



Self-assembly of rationally designed asymmetric amphiphilic monomers in water produced nanotube hydrogels in the presence of chemically denatured proteins (green fluorescent protein, carbonic anhydrase, and citrate synthase) at room temperature, which were able to encapsulate the proteins in the one-dimensional channel of the nanotube consisting of a monolayer membrane. Decreasing the concentrations of the denaturants induced refolding of part of the encapsulated proteins in the nanotube channel. Changing the pH dramatically reduced electrostatic attraction between the inner surface mainly covered with amino groups of the nanotube channel and the encapsulated proteins. As a result, the refolded proteins were smoothly released into the bulk solution without specific additive agents. This recovery procedure also transformed the encapsulated proteins from an intermediately refolding state to a completely refolded state. Thus, the nanotube hydrogels assisted the refolding of the denatured proteins and acted as artificial chaperones. Introduction of hydrophobic sites such as a benzyloxycarbonyl group and a *tert*-butoxycarbonyl group onto the inner surface of the nanotube channels remarkably enhanced the encapsulation and refolding efficiencies based on the hydrophobic interactions between the groups and the surface-exposed hydrophobic amino acid residues of the intermediates in the refolding process. Refolding was strongly dependent on the inner diameters of the nanotube channels. Supramolecular nanotechnology allowed us to not only precisely control the diameters of the nanotube channels but also functionalize their surfaces, enabling us to fine-tune the biocompatibility. Hence, these nanotube hydrogel systems should be widely applicable to various target proteins of different molecular weights, charges, and conformations.

KEYWORDS: self-assembly · nanotubes · nanospaces · hydrogels · proteins · refolding · chaperones

able to trap denatured proteins in their nanospaces. An elution procedure involving specific buffers that included additive agents allowed the release of the denatured proteins from the zeolites into bulk solutions, and the released proteins simultaneously refolded into their mature forms. The refolding mechanism in the nanogel system could also involve the release of the trapped proteins into the bulk

* Address correspondence to n-kameta@aist.go.jp.

Received for review March 8, 2012 and accepted May 10, 2012.

Published online May 22, 2012
10.1021/nn301041y

© 2012 American Chemical Society

solutions accompanied by the dissociation of the nanogel as a result of the addition of CDs. Although both systems were applicable to the refolding of various proteins, the obtained solutions of target proteins included the additive agents, complexes of the nanogel components with CDs, and unfolded proteins.

On the other hand, self-assembly of rationally designed amphiphilic molecules in water can produce well-defined, one-dimensional tubular structures.⁴⁴ Self-assembled nanotubes provide hydrophilic channels with 5–100 nm inner diameters, which can not only encapsulate oligo DNA, double-stranded DNA, and native proteins with folded structures^{45–50} but also protect the encapsulated biomaterials from chemically and thermally unfavorable conditions.⁵¹ We can control the release of the encapsulated guests into bulk solutions by using external stimuli such as pH, temperature, and light.⁵¹ Moreover, hierarchical aggregation and entanglement of the nanotubes in water enable us to construct hydrogels, which function as soft nanomaterials for medical, nano-, and nanobio-applications.^{52–57} Thus, the chemical and physical properties of the nanospaces and the nanotube channels are remarkably different from those of the nanospace materials as mentioned above, in that they have controllable diameters and functionalizable surfaces, respond to stimuli, and are biocompatible.

Here, we describe how nanotube hydrogels can serve as artificial chaperones for denatured proteins, that is, the encapsulation of denatured proteins in nanotube channels, refolding assistance of the encapsulated proteins, and the release/recovery of the refolded proteins without the addition of specific agents. We discuss the effects of interior hydrophobic groups and the diameter of the nanotube channels in the hydrogels on their chaperone abilities.

RESULTS AND DISCUSSION

We chose the asymmetric amphiphile **1** (Figure 1, base monomer) because it can form the nanotube hydrogel at room temperature in response to pH stimulus; that is, we can control the protonation state of the terminal amino groups.⁵³ The formation of the other nanotubes generally required heating to temperatures above the phase transition of each amphiphile used.⁴⁴ We previously found that binary self-assembly of **1** and the derivative **3** (Figure 1, functional monomer) bearing Alexa Fluor 546 (Molecular Probes) produced a nanotube consisting of a single monolayer (molecular monolayer) membrane lined by polyglycine-II-type hydrogen-bond networks among the triglycine moieties of **1** and **3** (Figure 1).^{58,59} The Alexa-immobilized nanotube could detect native green fluorescent protein (GFP) in the nanotube channel *via* fluorescence resonance energy transfer (FRET) from the encapsulated native GFP, which served as a

fluorescence donor, to the Alexa on the nanotube inner surface, which served as a fluorescence acceptor. The FRET mechanism can be used to directly monitor refolding from the denatured GFP, which lacks fluorescence (FRET off) to the folded GFP, which recovers its fluorescence (FRET on).

endo-Sensing for the Refolding of GFP. The hydrochloride salt of **1** (5.0 mg, 6.9 μ mol) and **3** (1.0 mg, 0.60 μ mol) were dissolved in water (1 mL) at pH 5. GFP (5–50 μ g, Aequorea Victoria, recombinant, MW = 28 000, Upstate) denatured with 6 M GdmCl was added in advance to the solution of **1** and **3** (Figure 2a), and the pH was then adjusted to 7 by the addition of NaOH. The resultant clear solution was instantly transformed to a hydrogel (Figure 2b). Scanning electron microscopic (SEM) observation of the xerogel (Figure 3a) revealed a tubular structure with well-defined open ends (Figure 3b). The penetration of the negative staining reagent, phosphotungstate, into the hollow cylinder demonstrated that the nanotubes have uniform dimensions (10 nm inner diameter and 3 nm membrane thickness; Supporting Information, Figure S1). We observed neither morphological changes nor decomposition of the nanotubes even though GdmCl was present in the system at high concentration (0.6 M), which usually disturbs hydrogen-bond formation in self-assembly. The obtained nanotube hydrogel (designated Alexa-hydrogel) was purified with water in a decantation manner to remove the non-encapsulated GFP located on the outside of the nanotubes (in the meshwork formed between the nanotubes) and to decrease the GdmCl concentration (Figure 2c). The encapsulation of the denatured GFP into the nanotube channel was completed as soon as the hydrogel formed (Supporting Information, Figure S2a), suggesting that encapsulation occurred during the process of nanotube formation. On the other hand, the addition of GFP to the preformed Alexa-hydrogel and subsequent washing with water allowed us to recover almost all of the added GFP. The preformed nanotube showed no ability to encapsulate the denatured GFP, having a larger volume than native GFP (Supporting Information, Figure S2b), whereas the 10 nm inner diameter of the nanotube channel was large enough to encapsulate the native GFP with a 3–4 nm size.⁵³ When the hydrogel formed in the presence of denatured GFP, the maximum amount of encapsulated GFP was 18 μ g (Supporting Information, Figure S2b).

Fluorescence spectroscopy indicated the occurrence of FRET, in which the fluorescence bands of GFP at 510 nm and of Alexa at 570 nm appeared over time (Supporting Information, Figure S3). The excitation wavelength at 450 nm was adaptable for the excitation of GFP, but never directly excited Alexa. This finding can be explained as follows: part of the encapsulated GFP that lacked fluorescence transformed into the refolded state in the nanotube channel. The completely refolded GFP recovered its original

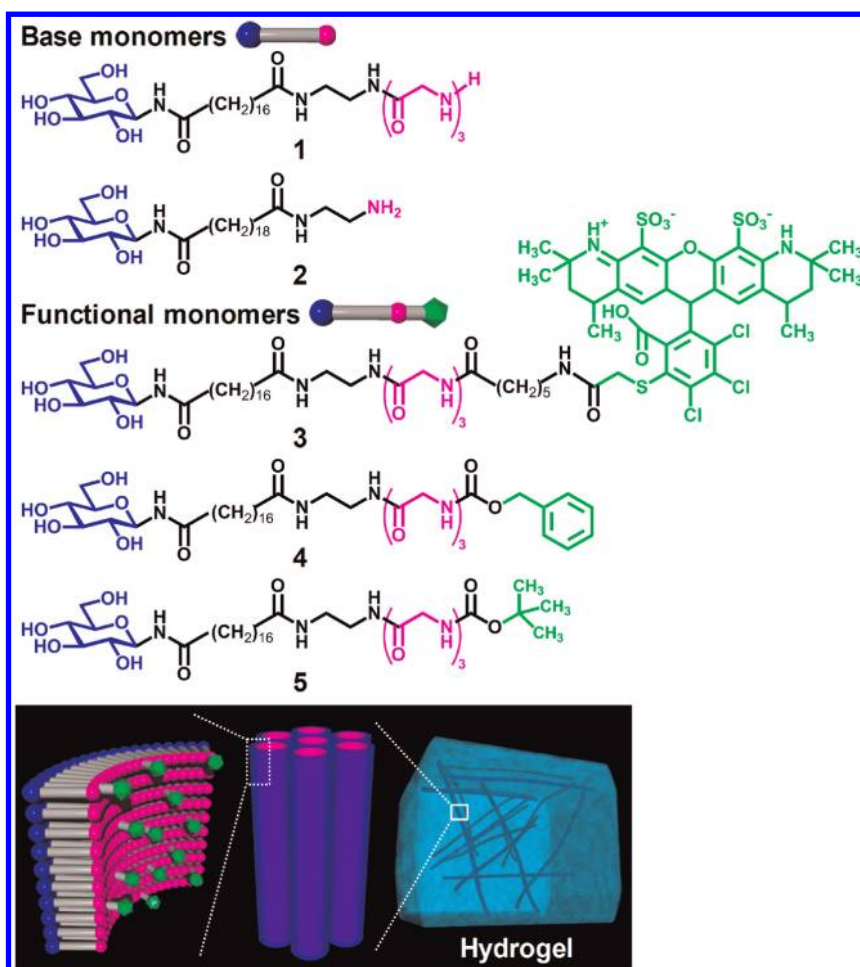


Figure 1. Structures of the base monomers 1 and 2 and functional monomers 3, 4, and 5. Schematic image of the hydrogels based on the nanotube network self-assembly of the base and functional monomers. The nanotubes consist of a molecular monolayer membrane, in which both monomers are packed in a parallel fashion.

fluorescence and illuminated the Alexa on the inner surface of the nanotube *via* the FRET process. Fluorescence microscopic observation clearly showed the strong fluorescence derived from the FRET phenomenon along the high-axial direction of the nanotubes in the hydrogel (Figure 3c). The refolding ratio of the encapsulated GFP in the nanotube channel was higher than that of the free GFP in the bulk solution, which was estimated by a general dilution method (Figure 4 and Table 1). Namely, the one-dimensional confined nanospace of the nanotube channel was able to assist in the refolding of the denatured GFP (Figure 2d, refolding process I).

To release and recover the encapsulated GFP, we added water adjusted to pH 7.0 and 7.8 (recovery solutions) to the hydrogel (Figure 2e). When the pH was 7.0, the FRET intensity in the nanotube hydrogel barely changed, and the recovery solution showed no fluorescence of the refolded GFP, even after 48 h. This result indicates that the encapsulated GFP stays in the Alexa-hydrogel. The nanotube channel had positively charged ammonium groups at pH 7.0 and preserved the negatively charged GFP (isoelectric point of the

native state: $pI = 4.7-5.1$)⁶⁰ *via* electrostatic attraction. When the pH was increased to 7.8, the FRET intensity in the Alexa-hydrogel decreased while the fluorescence intensity of the refolded GFP in the recovery solution increased. The dramatic reduction in electrostatic attraction, based on the deprotonation of almost all of the ammonium groups, enabled the Alexa-hydrogel to effectively release the refolded GFP into the recovery solution. The recovery profile, which was identical to the release profile, indicated a gentle rise from 0 to 16 h and then a relative steep curve from 20 to 36 h (Figure 5). On the other hand, the release profile of the pre-encapsulated native GFP in the nanotube channel indicated only the gently rising curve.^{58,59} The maximum value (71%) of the total refolding ratio in the recovery solution was larger than that (35%) of the refolding ratio in the nanotube channel prior to refolding process I (Figure 5 and Table 1), indicating that the incompletely refolded GFP in the nanotube channel transforms into the completely refolded state after release into the recovery solution (refolding process II, Figure 2e). Such refolding mechanisms have been shown in other artificial chaperone systems, in which the protein refolding was accompanied

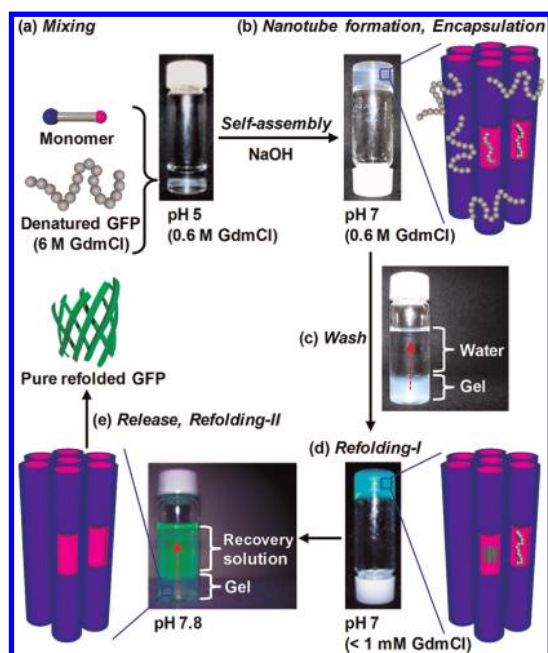


Figure 2. Refolding procedure of denatured GFP in the nanotube hydrogel. To emphasize the recovered green fluorescence of the refolded GFP, we used the nanotube hydrogel that self-assembles from the single component 1, without 3.

with the elution of the proteins from the nanospace of the artificial chaperones into bulk solutions by using specific additive agents.^{36–43} Since the present system did not require any additive agents to elute (release) the encapsulated proteins from the nanotube channel into the recovery solution, the obtainable refolded GFP in the recovery solution was very pure. Although the total refolding ratio did not reach 100% (Figure 5), the recovery solution included neither unfolded GFP nor aggregates, which remained in the nanotube channel.

We also confirmed that refolding no longer occurred after the first washing treatment with water to remove the nonencapsulated GFP from the outside of the nanotubes (Figure 2c). The outside of the nanotube, that is, the outer surface of the nanotube itself and the interstitial nanospaces consisting of the three-dimensional meshwork of the nanotubes, showed no chaperone ability. The chaperone abilities of liposomes have been shown to strongly depend on the surface charge and fluidity of the bilayer membrane walls, which are important for rational electrostatic and hydrophobic interactions with denatured proteins.^{7–9} In the present system, the nonionic hydroxy groups in the glucose residues on the outer surface and the long alkyl chains within the solid-state monolayer membrane wall of the nanotube barely interacted with the denatured GFP.

Effect of Hydrophobic Interactions on the Refolding of Carbonic Anhydrase (CAB). Since denatured proteins with the refolding-intermediate state are well-known to

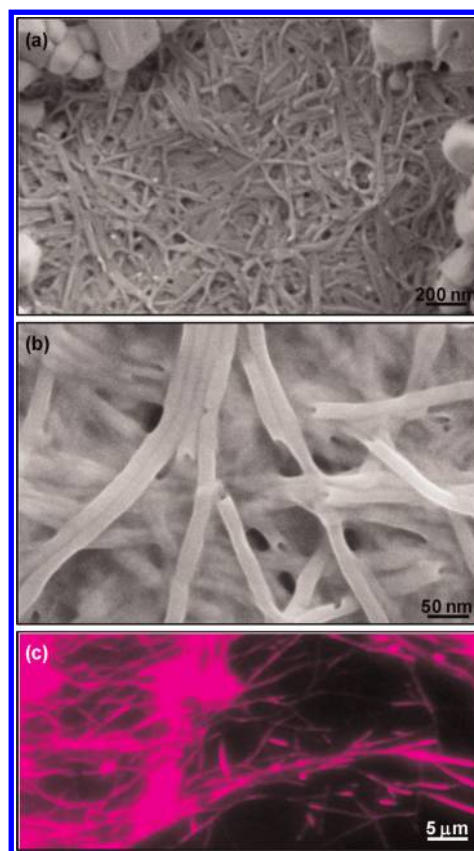


Figure 3. (a, b) SEM images of the nanotube xerogel prepared by lyophilization of the Alexa-hydrogel that encapsulated the denatured GFP (prior to being washed with water). The block objects are crystals of excess GdmCl (0.6 M). (c) Fluorescence microscopic image of the Alexa-hydrogel that encapsulated the refolded GFP. The fluorescence derives from FRET from the refolded GFP to the Alexa group on the inner surface of the nanotube.

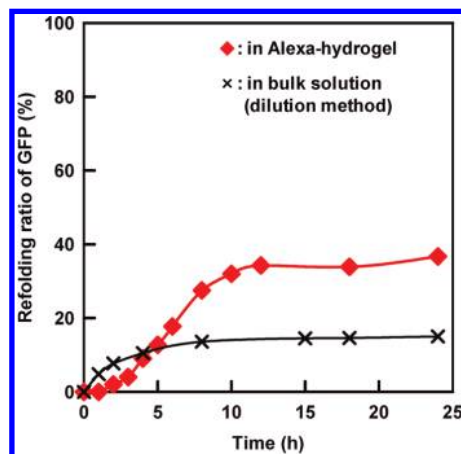


Figure 4. Time dependence of the refolding ratios of encapsulated GFP ($=18 \mu\text{g}$) in the nanotube channel of the Alexa-hydrogel or free GFP ($=18 \mu\text{g}$) in the bulk solution (dilution method).

have surface-exposed hydrophobic amino acid residues,⁶¹ we investigated the effect of hydrophobicity of the nanotube inner surface on the chaperone ability. Accordingly, we evaluated the chaperone

TABLE 1. Refolding Ratios of Denatured Proteins in the Nanotube Hydrogel and Dilution Method Systems^a

media for refolding	GFP		CAB		CS	
	refolding I	refolding I + II	refolding I	refolding I + II	refolding I	refolding I + II
Alexa-hydrogel	35%	71% (max.)				
H-hydrogel			38%	53% (max.)	0%	17% (max.)
LZ-hydrogel			44%	84% (max.)		
LBoc-hydrogel			46%	70% (max.)		
20-H-hydrogel	0%	0%	0%	0%	30%	62% (max.)
bulk (dilution method)		14%		16%		7%

^a Alexa-hydrogel: composed of **1** and **3**. H-hydrogel: composed of **1**. LZ-hydrogel: composed of **1** and **4**. LBoc-hydrogel: composed of **1** and **5**. 20-H-hydrogel: composed of **2**. GFP: green fluorescent protein. CAB: carbonic anhydrase. CS: citrate synthase.

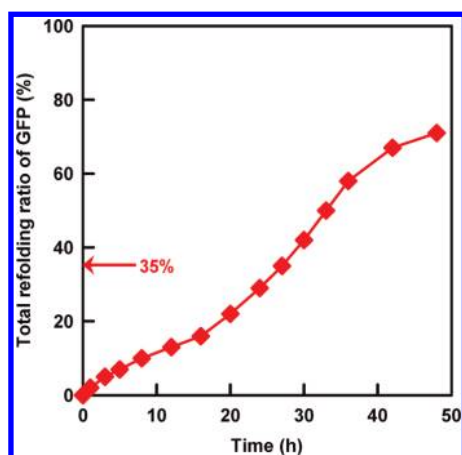


Figure 5. Time dependence of the total refolding ratio of the released GFP from the Alexa-hydrogel into the recovery solution. [Encapsulated GFP] = 18 μ g. Part (35%) of the encapsulated GFP was completely refolded in the nanotube channel (refolding process I).

abilities of both a nanotube hydrogel (abbreviated as LZ-hydrogel hereafter) composed of **1** and the derivative **4** bearing a benzyloxycarbonyl group and a nanotube hydrogel (abbreviated as LBoc-hydrogel hereafter) composed of **1** and the derivative **5** bearing a *tert*-butoxycarbonyl group. We compared their chaperone abilities with that of a nanotube hydrogel (abbreviated as H-hydrogel hereafter) composed of just **1**. CAB (from bovine, MW = 30 000, pI = 5.9, Sigma) was chosen as a target protein, because it has been widely studied in the artificial chaperone systems. Denatured CAB (5–50 μ g) together with 6 M GdmCl was added to an aqueous solution (1 mL) of **1** (5.0 mg, 6.9 μ mol) and **4** (0.57 mg, 0.69 μ mol) or to an aqueous solution (1 mL) of **1** (5.0 mg, 6.9 μ mol) and **5** (0.54 mg, 0.69 μ mol), or an aqueous solution (1 mL) of **1** (5.5 mg, 7.6 μ mol). Hydrogel formation, encapsulation, and washing were carried out in the same manner as described for the GFP–Alexa-hydrogel system.

The denatured CAB was more effectively encapsulated into the LZ-hydrogel (**1:4** = 91:9 mol %) and the LBoc-hydrogel (**1:5** = 91:9 mol %) than into the H-hydrogel (**1** = 100 mol %) as expected from the hydrophobic interactions between the hydrophobic groups

on the nanotube inner surface and the surface-exposed hydrophobic amino acid residues of the denatured CAB that was in the refolding-intermediate state (Figure 6a and Supporting Information, Figure S4). This result also suggests that the benzyloxycarbonyl group in the LZ-hydrogel interacts more strongly with the denatured CAB compared with the *tert*-butoxycarbonyl group in the LBoc-hydrogel. The refolding ratios of CAB in all of the nanotube hydrogel systems were higher than that in the general dilution method system (Figure 6b and Table 1), indicating that each nanotube channel in the hydrogels assists in the refolding process (refolding process I). Although the denatured CAB was stably encapsulated in the nanotube channels by the hydrophobic interactions and required more time to refold, both refolding ratios for the LZ-hydrogel and LBoc-hydrogel systems were comparable to that of the H-hydrogel system. However, further increases in the hydrophobicity of the nanotube inner surface decreased the refolding ratio. The encapsulated CAB in the LZ-hydrogel (**1:4** = 51:49 mol %) composed of **1** (2.8 mg, 3.9 μ mol) and **4** (3.0 mg, 3.7 μ mol) never transformed into the refolded state (Supporting Information, Figure S5).

To evaluate the chemical and thermal stabilities of the refolded CAB in the nanotube channel, we treated the nanotube hydrogels encapsulating the refolded CAB with a denaturant or with heat. The enzyme activity of the free CAB in the bulk solution was completely lost after incubation with 8 M urea for 1 h or when the temperature was elevated to the 70–85 $^{\circ}$ C range for 1 h, whereas over 90% of the enzyme activity of the encapsulated CAB in each nanotube channel was retained under the same conditions (Supporting Information, Figures S6 and S7). We previously showed that encapsulated GFP and encapsulated myoglobin in the nanotube channel retain their respective fluorescence and oxygen-binding activities under high denaturant concentrations and at high temperatures.^{53,58,59} Therefore, the higher stability of the encapsulated CAB can be attributed to the confinement effect^{62,63} based on rational fitting of the inner diameter (10 nm) of the nanotube to the size (3–4 nm) of the refolded CAB.

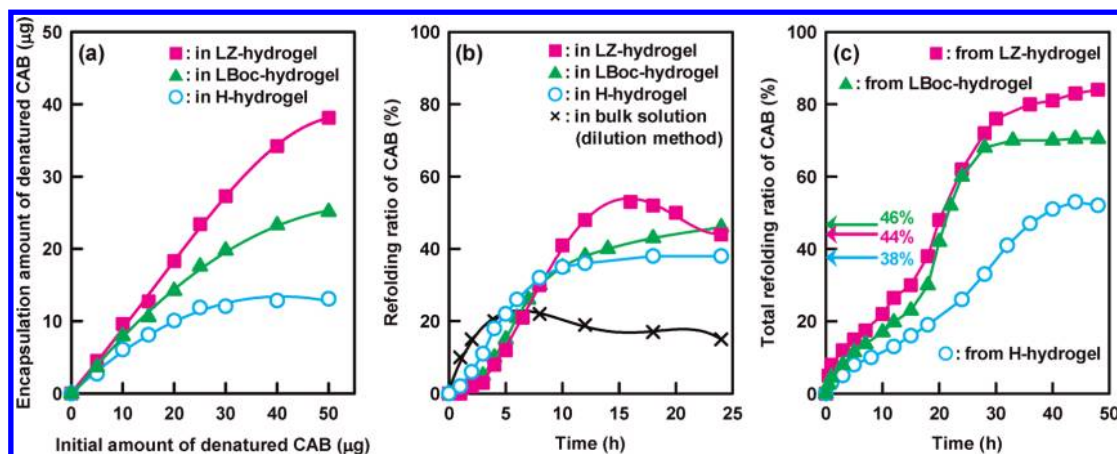


Figure 6. (a) Relationship between the initial amount of denatured CAB and the amount of encapsulated denatured CAB in the nanotube hydrogels. (b) Time dependence of the refolding ratio of the encapsulated CAB ($=13 \mu\text{g}$) in the nanotube channel of the hydrogels or the free CAB ($=13 \mu\text{g}$) in the bulk solution (dilution method). (c) Time dependence of the total refolding ratio of the CAB released from the nanotube hydrogels into the recovery solution. [Encapsulated CAB] = $13 \mu\text{g}$. Part (38%–46%) of the encapsulated CAB was completely refolded in the nanotube channel (refolding process I).

Such stabilization and protection of proteins by the nanotube channels *via* this confinement effect were independent of the functional groups on the inner surface of the nanotubes.

Release and recovery of the encapsulated CAB in the nanotube hydrogels were also achieved by pH control in the same manner as described for the GFP–Alexa-hydrogel system. The total refolding ratio consisted of the sum of the CAB refolded in the nanotube channel (refolding process I) and the CAB refolded upon release from the nanotube channel into the bulk solution (refolding process II). The maximum value of the total refolding ratios in the recovery solution were larger than the refolding ratio in the nanotube channel before the release procedure *via* refolding process I (Figure 6c and Table 1). We confirmed that the recovery solutions contained only completely refolded CAB that had enzyme activity and that the nanotube channels stored the unfolded CAB. The higher refolding ratios in the LZ-hydrogel and LBoc-hydrogel systems, compared with that in the H-hydrogel system (Figure 6c), can be attributed to the fact that the partial hydrophobic modification groups of the nanotube channels suppressed the adsorption of the hydrophilic CAB formed through refolding process I on the inner surface of the nanotube. Circular dichroism spectroscopy showed that the encapsulated CAB in the nanotube hydrogels, particularly the LZ- and LBoc-hydrogels, had an increased proportion of α -helix structure⁶⁴ (Figure S8). A similar conformational change was observed in encapsulated CAB that had an intermediately refolded state in the relative hydrophobic nanospace in nanogels acting as artificial chaperones.^{65,66} Thus, the relatively hydrophobic nanotube channels in the LZ- and LBoc-hydrogels should induce the formation of the intermediate state to allow complete refolding and acceleration of refolding process II.

Effect of Inner Diameters on the Refolding of Citrate Synthase (CS) and CAB. To clarify the effect of the inner diameters of the nanotubes on their chaperone abilities for different sized proteins, we employed a nanotube hydrogel (abbreviated as 20-H-hydrogel) formed by a network of nanotubes of 20 nm inner diameter composed of monomer **2**.⁵⁹ A homodimeric protein, CS (from porcine heart, MW = 100 000, pI = 6.6, Sigma), was chosen as the target protein, because its molecular weight is more than three times that of CAB. In fact, the size of native CS, $7.5 \times 6.0 \times 9.0 \text{ nm}$,⁶⁷ is larger than that (3–4 nm) of native CAB.⁶⁸

Encapsulation of CS or CAB was carried out by the formation of the 20-H-hydrogel by self-assembly of **2** (5.0 mg, $8.6 \mu\text{mol}$) in water (1 mL) in the presence of CS (5–50 μg) or CAB (5–50 μg) denatured by 6 M GdmCl (Figure 7a and d, see Methods section and Supporting Information, Figure S9). The washing and recovery procedures were as described for the H-hydrogel system except for the use of ethylenediamine-*N,N,N',N'*-tetraacetic acid (EDTA) and dithiothreitol (DTT) in the case of CS. The 20-H-hydrogel assisted not only in the refolding of the encapsulated CS in the nanotube channel with the 20 nm inner diameter (refolding process I) but also in the refolding of the released CS into the recovery solution (refolding process II) (Figure 7b and c). On the other hand, the 20-H-hydrogel showed no chaperone ability for CAB (Figure 7e, f and Table 1). Circular dichroism spectroscopy suggested that the nanotube channel with the 20 nm inner diameter induced aggregation of the encapsulated CAB accompanied by destruction of its α -helical structure, whereas the nanotube channel with the 10 nm inner diameter prevented aggregation (Supporting Information, Figure S10). This acceleration of CAB aggregation was probably due to the loose

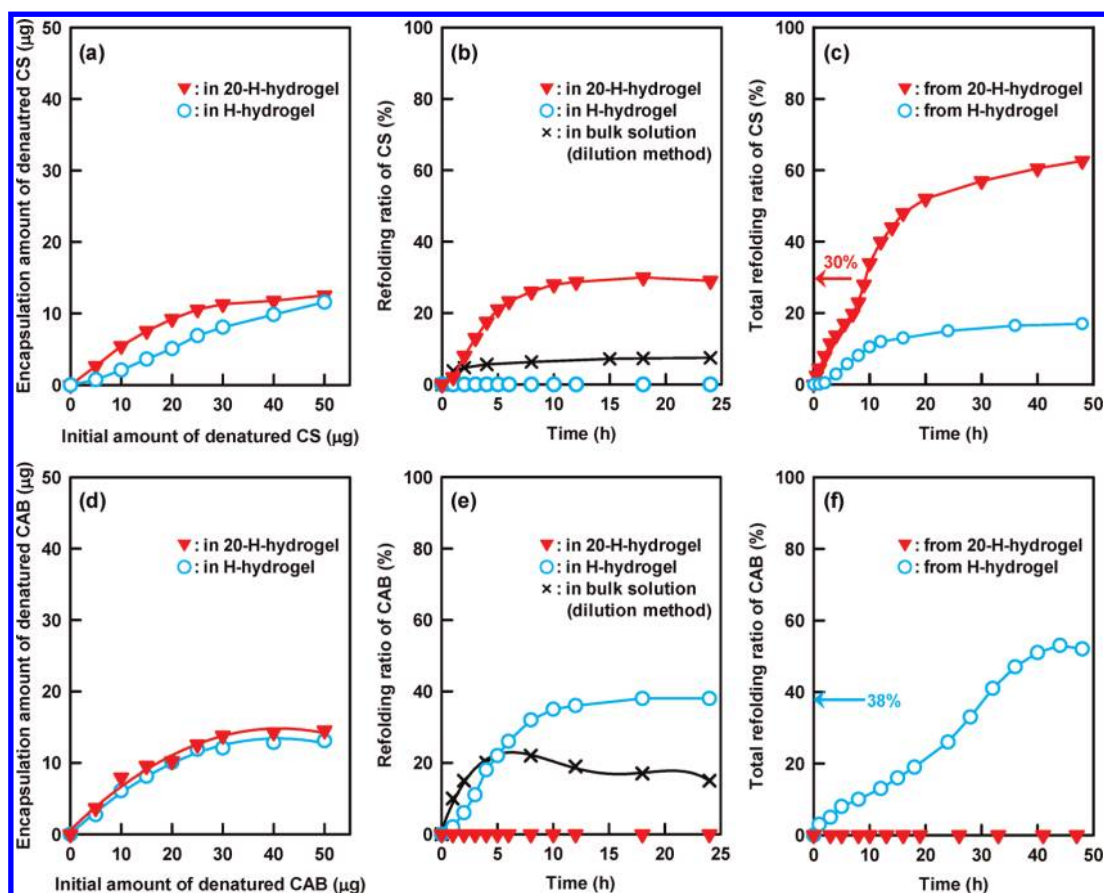


Figure 7. (a) Relationship between the initial amount of denatured CS and the amount of encapsulated denatured CS in the nanotube hydrogels. (b) Time dependence of the refolding ratio of the encapsulated CS ($=13 \mu\text{g}$) in the nanotube channel of the hydrogels or the free CS ($=13 \mu\text{g}$) in the bulk solution (dilution method). (c) Time dependence of the total refolding ratio of the CS released from the nanotube hydrogel into the recovery solution. [Encapsulated CS] = $13 \mu\text{g}$. In the case of the 20-H-hydrogel, part (30%) of the encapsulated CS was completely refolded in the nanotube channel (refolding process I). (d) Relationship between the initial amount of denatured CAB and the amount of encapsulated denatured CAB in the nanotube hydrogels. (e) Time dependence of the refolding ratio of the encapsulated CAB ($=15 \mu\text{g}$) in the nanotube channel of the hydrogels or the free CAB ($=15 \mu\text{g}$) in the bulk solution (dilution method). (f) Time dependence of the total refolding ratio of the CAB released from the nanotube hydrogel into the recovery solution. [Encapsulated CAB] = $15 \mu\text{g}$. In the case of the H-hydrogel, part (38%) of the encapsulated CAB was completely refolded in the nanotube channel (refolding process I).

geometry of the nanotube channel with the 20 nm inner diameter relative to the size of CAB, since the 20-H-hydrogel inhibited the refolding of GFP, which has a similar molecular weight to that of CAB (Supporting Information, Figure S11).

Although the H-hydrogel encapsulated CS (Figure 7a), the encapsulated CS was barely refolded in the nanotube channel *via* refolding process I (Figure 7b and Table 1). The total refolding efficiency of the released CS in the bulk solution was also lower than that of the released CAB in the bulk solution (open circle plots in Figure 7c and f and Table 1). The nanotube channel with the 10 nm inner diameter in the H-hydrogel was likely too small to assist in the refolding of CS.

In conclusion, we successfully constructed an artificial chaperone based on nanotube hydrogels. The hydrogels not only could encapsulate chemically denatured proteins in nanotube channels but also

assisted in transforming the proteins into their refolded states. Hydrophobic interactions between nanotube channels that were modified with hydrophobic groups and the surface-exposed hydrophobic amino acid residues of denatured proteins in the intermediately refolded state remarkably enhanced the efficiency of encapsulation and refolding. Size balance between the nanotube channel and the proteins was also important for refolding efficiency. The recovery of pure refolded proteins from nanotube hydrogels *via* pH stimulus has not previously been achieved with artificial chaperone systems, because in these previous systems the refolded proteins coexist with specific additive agents, the artificial chaperones themselves, decomposed materials, and unfolded proteins. The precise design of the amphiphilic molecules and self-assembly nanotechnology enabled us to judiciously control the inner diameter size and selectively functionalize the inner surface (with cationic, anionic,

nonionic, and hydrophobic groups) of the nanotubes. These nanotube hydrogel systems should thus be

widely applicable to various target proteins of different molecular weights, charges, and conformations.

METHODS

Synthesis of the Functional Monomer 4. The precursor *N*-(2-aminoethyl)-*N'*-(2,3,4,6-tetra-*O*-acetyl- β -*D*-glucopyranosyl)octadecanedi-*amide* was synthesized as reported previously.⁵³ The precursor was coupled with Z-GlyGlyGly-OSu (Bachem) in dimethylformamide at room temperature and purified by recrystallization. Removal of all acetyl groups by methanolysis quantitatively gave **4**. ¹H NMR (400 MHz, DMSO-*d*₆/D₂O = 98:2, v/v, 60 °C): δ 7.35 (m, 5H, Phe), 5.03 (s, 2H; -CH₂-Phe), 4.69 (t, 1H; H-1), 3.75 (d, 2H; NCH₂C=O), 3.67 (s, 2H; NCH₂C=O), 3.65 (d, 2H; NCH₂C=O), 3.63 (m, 1H; H-6), 3.40 (m, 1H; H-6), 3.16 (m, 1H; H-4), 3.08 (m, 4H; NCH₂CH₂N), 3.05 (m, 3H; H-2, H-3, H-5), 2.04 (m, 4H; CH₂C=O), 1.47 (m, 4H; CH₂), 1.24 (m, 24H; CH₂). ESI-MS (*m/z*): 823.5 [M + H]⁺. Anal. Calcd for C₄₀H₆₈N₆O₁₂: C 58.38, H 8.08, N 10.21. Found: C 58.69, H 8.90, N 12.02.

Synthesis of the Functional Monomer 5. The precursor *N*-(2-aminoethyl)-*N'*-(2,3,4,6-tetra-*O*-acetyl- β -*D*-glucopyranosyl)octadecanedi-*amide* was coupled with Boc-GlyGlyGly-OSu (Bachem) in dimethylformamide at room temperature and purified by recrystallization. Removal of all acetyl groups by methanolysis quantitatively gave **5**. ¹H NMR (400 MHz, DMSO-*d*₆/D₂O = 98:2, v/v, 60 °C): δ 4.69 (t, 1H; H-1), 3.75 (d, 2H; NCH₂C=O), 3.67 (s, 2H; NCH₂C=O), 3.65 (d, 2H; NCH₂C=O), 3.63 (m, 1H; H-6), 3.40 (m, 1H; H-6), 3.16 (m, 1H; H-4), 3.08 (m, 4H; NCH₂CH₂N), 3.05 (m, 3H; H-2, H-3, H-5), 2.04 (m, 4H; CH₂C=O), 1.47 (m, 4H; CH₂), 1.38 (s, 9H, CH₃), 1.24 (m, 24H; CH₂). ESI-MS (*m/z*): 789.5 [M + H]⁺. Anal. Calcd for C₃₇H₆₈N₆O₁₂: C 56.33, H 8.69, N 10.65. Found: C 56.81, H 8.75, N 10.59.

Formation of the 20-H-Hydrogel. Prior to self-assembly in water, the hydrochloride salt of monomer **2** was changed from a powder to a film by dissolving it in *N,N*-dimethylformamide and evaporating the solvent at 80 °C *in vacuo*. The film was dispersed in an aqueous solution of the denatured proteins and 0.6 M GdmCl at pH 7 (adjusted with NaOH) at room temperature. For CS, the aqueous solution also included 0.75 mM EDTA and 0.4 mM DTT. The resultant aqueous solution completely transformed into the hydrogel after standing for 1 h.

SEM Observation. The nanotube hydrogels formed in the presence of the denatured proteins were lyophilized, and the resultant xerogels were then dropped onto the grid. The nanotubes were observed with a scanning electron microscope (Carl Zeiss, FE-SEM Supra 40) at 1 kV equipped with a chamber SE detector (SE2 mode).

TEM Observation. The aqueous dispersion of the nanotube hydrogel containing the encapsulating proteins was dropped onto a carbon grid and dried by standing at room temperature. The nanotubes, negatively stained with a phosphotungstate solution (2 wt %, pH adjusted to 9 with NaOH), were observed with a transmission electron microscope (Hitachi, H-7000) at 75 kV.

Fluorescence Microscopic Observation. Fluorescence microscopic observations of the nanotube hydrogel that encapsulated the refolded GFP were achieved with an inverted microscope (Olympus IX71) equipped with a CCD camera (Hamamatsu ORCA-ER). The excitation optical source was prepared by means of a high-pressure mercury lamp (100 W, Olympus BH2-REL-T3) and a fluorescence mirror unit (Olympus U-MGFPHQ: excitation filter 470–495 HQ, Absorption filter 570–625 HQ, dichroic mirror 485).

Denaturation of Proteins and Refolding of the Denatured Proteins by the Dilution Method. Native GFP or CAB was added to the aqueous solution containing 6 M GdmCl and Tris-sulfate buffer (pH 7.5). Native CS was added to the aqueous solution that included 6 M GdmCl, 7.5 mM EDTA, 40 mM DTT, and Tris-HCl buffer (pH 7.6). The resultant solutions were left for 24 h at room temperature. The formation of the denatured proteins was confirmed by means of circular dichroism spectroscopy. The denatured proteins were diluted 1000-fold in refolding buffer (Tris-sulfate or Tris-HCl) and stored for 1–25 h at 25 °C.

Encapsulation and Refolding Ratio of GFP. The concentrations of the denatured and refolded GFP were determined by using the BCA protein assay kit (Pierce). The encapsulation amount of denatured GFP (in Figure S2) was directly calculated from the concentration of encapsulated GFP in the nanotube hydrogel. We also calculated the concentration of nonencapsulated GFP that was recovered as a result of the washing procedure and confirmed that the sum of the encapsulated and nonencapsulated GFP concentrations is equal to the initial concentration of GFP. The release ratio of GFP was calculated from the concentration of the released GFP in the bulk solution and the concentration of the GFP that remained in the nanotube hydrogel. The percentage of refolded GFP in the nanotube channel was estimated by comparing the FRET intensity at 570 nm of the Alexa in the nanotube that encapsulated the refolded GFP with that of the Alexa in the nanotube that encapsulated the native GFP at a given concentration. The percentage of refolded GFP in the recovery solution was estimated by comparing the fluorescence intensity at 510 nm of the refolded GFP with that of the native GFP at a given concentration.

Encapsulation and Refolding Ratio of CAB. The concentrations of the denatured and refolded CAB were determined by using the BCA protein assay kit. The encapsulation amount of denatured CAB (in Figures 6a and 7d) was directly calculated from the concentration of encapsulated CAB in the nanotube hydrogel. We also calculated the concentration of nonencapsulated CAB that was recovered as a result of the washing procedure and confirmed that the sum of the encapsulated and nonencapsulated CAB concentrations is equal to the initial concentration of CAB. The release ratio of CAB was calculated from the concentration of released CAB in the bulk solution and the concentration of CAB that remained in the nanotube hydrogel. The percentage of refolded CAB was estimated by comparing the enzyme activity of the refolded CAB with that of native CAB at a given concentration. The enzyme activity was evaluated by pNPA hydrolysis assay.⁶⁹ The pNPA solution was added to the encapsulated CAB in the nanotube hydrogels or to the CAB in the recovery solutions. The increase in absorbance at 400 nm was measured as a function of time.

Encapsulation and Refolding Ratio of CS. The concentrations of the denatured and refolded CS were determined by using the BCA protein assay kit. The encapsulation amount of denatured CS (in Figure 7a) was directly calculated from the concentration of encapsulated CS in the nanotube hydrogel. We also calculated the concentration of nonencapsulated CS that was recovered as a result of the washing procedure and confirmed that the sum of the encapsulated and nonencapsulated CS concentrations is equal to the initial concentration of CS. The release ratio of CS was calculated from the concentration of released CS in the bulk solution and the concentration of CS that remained in the nanotube hydrogel. The percentage of refolded CS was estimated by comparing the enzyme activity of the refolded CS with that of native CS at a given concentration. The enzyme activity was evaluated by using the acetyl-CoA assay.⁷⁰ An aqueous solution of 5,5'-dithiobis(2-nitrobenzoic acid), acetyl-CoA, and oxaloacetic acid was added to the encapsulated CS in the nanotube hydrogels or to the CS in the recovery solutions. The increase in absorbance at 412 nm was measured as a function of time.

Spectroscopic Measurements. Fluorescence, UV/vis, and circular dichroism spectra were recorded by using an F-4500 spectrophotometer (Hitachi) equipped with a DCI temperature control (HAAKE), a U-3300 spectrophotometer (Hitachi) equipped with a BU150A temperature control (YAMATO), and a J-820 spectropolarimeter (JASCO) equipped with a PTC-423 L temperature control (JASCO), respectively.

Conflict of Interest: The authors declare no competing financial interest.

Supporting Information Available: TEM image of the nanotubes formed by binary self-assembly of **1** and **3** in the presence of denatured GFP. Encapsulation equilibrium and amount of

GFP in the nanotube hydrogel. Fluorescence spectra of the FRET phenomenon from the refolded GFP to the Alexa group on the nanotube inner surface. Encapsulation equilibrium of CAB in the nanotube hydrogels. Refolding ratio of CAB in the LZ-hydrogel composed of **1** and **4** at different ratios. Chemical and thermal stabilities of the refolded CAB in the nanotube hydrogels. Circular dichroism spectra of the encapsulated CAB in the nanotube hydrogels. TEM image of the nanotubes formed by self-assembly of **2** in the presence of denatured CS. Circular dichroism spectra of the encapsulated CAB in the nanotube hydrogels. Refolding ratio of GFP in the 20-H-hydrogel system. These materials are available free of charge via the Internet at <http://pubs.acs.org>.

REFERENCES AND NOTES

- Rudolph, R.; Lile, H. In Vitro Folding of Inclusion Body Proteins. *FASEB J.* **1996**, *10*, 49–56.
- Chow, M. K.; Amin, A. A.; Fulton, K. F.; Fernando, T.; Kamau, L.; Batty, C.; Louca, M.; Ho, S.; Whisstock, J. C.; Bottomley, S. P.; Buckle, A. M. The Refold Database: a Tool for the Optimization of Protein Expression and Refolding. *Nucleic Acids Res.* **2006**, *34*, D207–212.
- Tandon, S.; Horowitz, P. M. Detergent-Assisted Refolding of Guanidinium Chloride-Denatured Rhodanese - The Effect of Lauryl Maltoside. *J. Biol. Chem.* **1986**, *261*, 5615–5618.
- Zardeneta, G.; Horowitz, P. M. Prospective - Detergent, Liposome, and Micelle-Assisted Protein Refolding. *Anal. Biochem.* **1994**, *223*, 1–6.
- Hashimoto, Y.; Ono, T.; Goto, M.; Hatton, A. Protein Refolding by Reversed Micelles Utilizing Solid-Liquid Extraction Technique. *Biotechnol. Bioeng.* **1998**, *57*, 620–623.
- Morimoto, N.; Ogino, N.; Narita, T.; Akiyoshi, K. Enzyme-Responsive Artificial Chaperone System with Amphiphilic Amylose Primer. *J. Biotechnol.* **2009**, *140*, 246–249.
- Kuboi, R.; Yoshimoto, M.; Walde, P.; Luisi, P. L. Refolding of Carbonic Anhydrase Assisted by 1-Palmitoyl-2-Oleoyl-sn-Glycero-3-Phosphocholine Liposomes. *Biotechnol. Prog.* **1997**, *13*, 828–836.
- Yoshimoto, M.; Kuboi, R. Oxidative Refolding of Denatured Reduced Lysozyme Utilizing the Chaperone-Like Function of Liposomes and Immobilized Liposome Chromatography. *Biotechnol. Prog.* **1999**, *15*, 480–487.
- Kuboi, R.; Mawatari, T.; Yoshimoto, M. Oxidative Refolding of Lysozyme Assisted by Negatively Charged Liposomes: Relationship with Lysozyme-Mediated Fusion of Liposomes. *J. Biosci. Bioeng.* **2000**, *90*, 14–19.
- Connolly, S. A.; Leser, G. P.; Yin, H.-S.; Jardetzky, T. S.; Lamb, R. A. Refolding of a Paramyxovirus F Protein from Prefusion to Postfusion Conformations Observed by Liposome Binding and Electron Microscopy. *Proc. Natl. Acad. Sci. U. S. A.* **2006**, *103*, 17903–17908.
- Geng, X.; Wang, C. Protein Folding Liquid Chromatography and Its Recent Developments. *J. Chromatogr. B* **2007**, *849*, 69–80.
- Kuboi, R.; Morita, S.; Ota, H.; Umakoshi, H. Protein Refolding Using Stimuli-Responsive Polymer-Modified Aqueous Two-Phase Systems. *J. Chromatogr. B* **2000**, *743*, 215–223.
- Yoshimoto, N.; Hashimoto, T.; Felix, M. M.; Umakoshi, H.; Kuboi, R. Artificial Chaperone-Assisted Refolding of Bovine Carbonic Anhydrase Using Molecular Assemblies of Stimuli-Responsive Polymers. *Biomacromolecules* **2003**, *4*, 1530–1538.
- Shimizu, H.; Fujimoto, K.; Kawaguchi, H. Refolding of Protein Using Thiol-Carrying Latex Particles. *Colloid Surf. A* **1999**, *153*, 421–427.
- Shimizu, H.; Fujimoto, K.; Kawaguchi, H. Renaturation of Reduced Ribonuclease a with a Microsphere-Induced Refolding System. *Biotechnol. Prog.* **2000**, *16*, 248–253.
- Simard, J. M.; Szymanski, B.; Erdogan, B.; Rotello, V. M. Control of Substrate Selectivity Through Complexation and Release of α -Chymotrypsin from Gold Nanoparticle Surfaces. *J. Biomed. Nanotechnol.* **2005**, *1*, 341–344.
- Cavaliere, F.; Chiessi, E.; Paradossi, G. Chaperone-Like Activity of Nanoparticles of Hydrophobized Poly(vinyl alcohol). *Soft Matter* **2007**, *6*, 718–724.
- Wu, X.; Narsimhan, G. Effect of Surface Concentration on Secondary and Tertiary Conformational Changes of Lysozyme Adsorbed on Silica Nanoparticles. *Biochim. Biophys. Acta* **2008**, *1784*, 1694–1701.
- De, M.; Rotello, V. M. Synthetic “Chaperones”: Nanoparticle-Mediated Refolding of Thermally Denatured Proteins. *Chem. Commun.* **2008**, 3504–3506.
- Raghava, S.; Singh, P. K.; Rao, A. R.; Dutta, V.; Gupta, M. N. Nanoparticles of Unmodified Titanium Dioxide Facilitate Protein Refolding. *J. Mater. Chem.* **2009**, *19*, 2830–2834.
- Saenger, W.; Jacob, J.; Gessler, K.; Steiner, T.; Hoffmann, D.; Sanbe, H.; Koizumi, K.; Smith, S. M.; Takaha, T. Structures of the Common Cyclodextrins and Their Larger Analogues Beyond the Doughnut. *Chem. Rev.* **1998**, *30*, 1787–1802.
- Sundari, C. S.; Raman, B.; Balasubramanian, D. Artificial Chaperoning of Insulin, Human Carbonic Anhydrase and Hen Egg Lysozyme Using Linear Dextrin Chains - a Sweet route to the Native State of Globular Proteins. *FEBS Lett.* **1999**, *443*, 215–219.
- Machida, S.; Ogawa, S.; Shi, X. H.; Takaha, T.; Fujii, K.; Hayashi, K. Cycloamylose as an Efficient Artificial Chaperone for Protein Refolding. *FEBS Lett.* **2000**, *486*, 131–135.
- Lu, D.; Zhang, K.; Liu, Z. Protein Refolding Assisted by an Artificial Chaperone Using Temperature Stimuli Responsive Polymer as the Stripper. *Biochem. Eng. J.* **2005**, *25*, 141–149.
- Laslo, A. C.; Ganea, E.; Obinger, C. Refolding of Hexameric Porcine Leucine Aminopeptidase Using a Cationic Detergent and Dextrin-10 as Artificial Chaperones. *J. Biotechnol.* **2009**, *140*, 162–168.
- Daugherty, D. L.; Rozema, D.; Hanson, P. E.; Gellman, S. H. Artificial Chaperone-Assisted Refolding of Citrate Synthase. *J. Biol. Chem.* **1998**, *273*, 33961–33971.
- Mannen, T.; Yamaguchi, S.; Honda, J.; Sugimoto, S.; Nagamune, T. Expanded-Bed Protein Refolding Using a Solid-Phase Artificial Chaperone. *J. Biosci. Bioeng.* **2001**, *91*, 403–408.
- Li, J. J.; Venkataramana, M.; Sanyal, S.; Janson, J. C.; Su, Z. G. Immobilized β -Cyclodextrin Polymer Coupled to Agarose Gel Properly Refolding Recombinant Staphylococcus Aureus Elongation Factor-G in Combination with Detergent Micelle. *Protein Expression Purif.* **2006**, *45*, 72–79.
- Esmaili, M. A.; Yazdanparast, R. Solid-Phase Assisted Refolding of Carbonic Anhydrase using β -Cyclodextrin-Polyurethane Polymer. *Protein J.* **2008**, *27*, 334–342.
- Chen, S.; Roseman, A. M.; Hunter, A. S.; Wood, S. P.; Burston, S. G.; Ranson, N. A.; Clarke, A. R.; Saibil, H. R. Location of a Folding Protein and Shape Changes in GROEL-GROES Complexes Imaged by Cryoelectron Microscopy. *Nature* **1994**, *371*, 261–264.
- Hunt, J. F.; Weaver, A. J.; Landry, S. J.; Gierasch, L.; Deisenhofer, J. The Crystal Structure of the GroES Co-Chaperonin at 2.8 Angstrom Resolution. *Nature* **1996**, *379*, 37–45.
- Ellis, R. J. Proteins as Molecular Chaperones. *Nature* **1987**, *328*, 378–379.
- Mayhew, M.; Silva, A. C. R.; Martin, J.; Erdjument-Bromage, H.; Tempst, P.; Hartl, F. U. Protein Folding in the Central Cavity of the GroEL-GroES Chaperonin Complex. *Nature* **1996**, *379*, 420–426.
- Taguchi, H.; Ueno, T.; Tadakuma, H.; Yoshida, M.; Funatsu, T. Single-Molecule Observation of Protein-Protein Interactions in the Chaperonin System. *Nat. Biotechnol.* **2001**, *19*, 861–865.
- Song, J.-L.; Jun, J. L.; Huang, Y.-S.; Chuang, D. T. Encapsulation of an 86-kDa Assembly Intermediate inside the Cavities of GroEL and Its Single-Ring Variant SR1 by GroES. *J. Biol. Chem.* **2003**, *278*, 2515–2521.
- Ravindra, R.; Zhao, S.; Gies, H.; Winter, R. Protein Encapsulation in Mesoporous Silicate: The Effects of Confinement on Protein Stability, Hydration, and Volumetric Properties. *J. Am. Chem. Soc.* **2004**, *126*, 12224–12225.
- Chiku, H.; Kawai, A.; Ishibashi, T.; Takehara, M.; Yanai, T.; Mizukami, F.; Sakaguchi, K. A Novel Protein Refolding Method Using a Zeolite. *Anal. Biochem.* **2006**, *348*, 307–314.

38. Wang, X.; Lu, D.; Austin, R.; Agarwal, A.; Mueller, L. J.; Liu, Z.; Wu, J.; Feng, P. Protein Refolding Assisted by Periodic Mesoporous Organosilicas. *Langmuir* **2007**, *23*, 5735–5739.
39. Togashi, H.; Nara, T.; Sekikawa, C.; Kawakami, M.; Yaginuma, N.; Tsunoda, T.; Sakaguchi, K.; Mizukami, F. Refolding of Lactate Dehydrogenase by Zeolite Beta. *Biotechnol. Prog.* **2009**, *25*, 200–206.
40. Nara, T. Y.; Togashi, H.; Sekikawa, C.; Sakaguchi, K.; Mizukami, F.; Tsunoda, T. High-Throughput Protein Refolding Screening Method Using Zeolite. *Biotechnol. Prog.* **2009**, *25*, 1071–1077.
41. Nara, T. Y.; Togashi, H.; Sekikawa, C.; Kawakami, M.; Yaginuma, N.; Sakaguchi, K.; Mizukami, F.; Tsunoda, T. Use of Zeolite to Refold a Disulfide-Bonded Protein. *Colloid Surf. B* **2009**, *68*, 68–73.
42. Nabati, F.; Habibi-Rezaei, M.; Amanlou, M.; Moosavi-Movahedi, A. A. Dioxane Enhanced Immobilization of Urease on Alkyl Modified Nano-Porous Silica Using Reversible Denaturation Approach. *J. Mol. Catal. B* **2011**, *70*, 17–22.
43. Review: Sasaki, Y.; Akiyoshi, K. Nanogel Engineering for New Nanobiomaterials: From Chaperoning Engineering to Biomedical Applications. *Chem. Rec.* **2010**, *10*, 366–376.
44. Review: Shimizu, T.; Masuda, M.; Minamikawa, H. Supramolecular Nanotube Architectures Based on Amphiphilic Molecules. *Chem. Rev.* **2005**, *105*, 1401–1443.
45. Review: Guo, X.; Matsui, H. Peptide-Based Nanotubes and Their Applications in Bionanotechnology. *Adv. Mater.* **2005**, *17*, 2037–2050.
46. Review: Shimizu, T. Self-Assembled Lipid Nanotube Hosts: The Dimension Control for Encapsulation of Nanometer-Scale Guest Substances. *J. Polym. Sci. Part A* **2006**, *44*, 5137–5152.
47. Review: Fang, J. Ordered Arrays of Self-Assembled Lipid Tubules: Fabrication and Applications. *J. Mater. Chem.* **2007**, *17*, 3479–3484.
48. Review: Shimizu, T. Self-assembled Organic Nanotubes: Toward Attoliter Chemistry. *J. Polym. Sci. Part A* **2008**, *46*, 2601–2611.
49. Review: Zhou, Y.; Shimizu, T. lipid Nanotubes: A Unique Template to Create Diverse One-Dimensional Nanostructures. *Chem. Mater.* **2008**, *20*, 625–633.
50. Review: Jung, J. H.; Parka, M.; Shinkai, S. Fabrication of Silica Nanotubes by Using Self-Assembled Gels and Their Applications in Environmental and Biological Fields. *Chem. Soc. Rev.* **2010**, *39*, 4286–4302.
51. Review: Kameta, N.; Minamikawa, H.; Masuda, M. Supramolecular Organic Nanotubes: How to Utilize the Inner Nanospace and the Outer Space. *Soft Matter* **2011**, *7*, 4539–4561.
52. Yang, Z.; Liang, G.; Wang, L.; Xu, B. Using a Kinase/Phosphatase Switch to Regulate a Supramolecular Hydrogel and Forming the Supramolecular Hydrogel in Vivo. *J. Am. Chem. Soc.* **2006**, *128*, 3038–3043.
53. Kameta, N.; Yoshida, K.; Masuda, M.; Shimizu, T. Supramolecular Nanotube Hydrogels: Remarkable Resistance Effect of Confined Proteins to Denaturants. *Chem. Mater.* **2009**, *21*, 5892–5898.
54. Zhang, L.; Rakotondradany, F.; Myles, A. J.; Fenniri, H.; Webster, T. J. Arginine-Glycine-Aspartic Acid Modified Rosette Nanotube-Hydrogel Composites for Bone Tissue Engineering. *Biomaterials* **2009**, *30*, 1309–1320.
55. Orbach, R.; Adler-Abramovich, L.; Zigerson, S.; Mironi-Harpaz, I.; Seliktar, D.; Gazit, E. Self-Assembled Fmoc-Peptides as a Platform for the Formation of Nanostructures and Hydrogels. *Biomacromolecules* **2009**, *10*, 2646–2651.
56. Amdursky, N.; Gazit, E.; Rosenman, G. Quantum Confinement in Self-Assembled Bioinspired Peptide Hydrogels. *Adv. Mater.* **2010**, *22*, 2311–2315.
57. Review: Cui, H. G.; Webber, M. J.; Stupp, S. I. Self-Assembly of Peptide Amphiphiles: From Molecules to Nanostructures to Biomaterials. *Biopolymers* **2010**, *94*, 1–18.
58. Kameta, N.; Masuda, M.; Mizuno, G.; Morii, N.; Shimizu, T. Supramolecular Nanotube endo Sensing for a Guest Protein. *Small* **2008**, *4*, 561–565.
59. Kameta, N.; Minamikawa, H.; Someya, Y.; Yui, H.; Masuda, M.; Shimizu, T. Confinement Effect of Organic Nanotubes Toward Green Fluorescent Protein (GFP) Depending on the Inner Diameter Size. *Chem.—Eur. J.* **2010**, *16*, 4217–4223.
60. Ward, W. W. Biochemical and Physical Properties of Green Fluorescent Protein. In *Green Fluorescent Protein: Properties, Applications, and Protocols*; Chalfie, M., Kain, S. R., Eds.; Wiley Interscience, 2006; p 43.
61. Chandler, D. Interfaces and the Driving Force of Hydrophobic Assembly. *Nature* **2005**, *437*, 640–647.
62. Review: Hudson, S.; Cooney, J.; Magner, E. Proteins in Mesoporous Silicates. *Angew. Chem., Int. Ed.* **2008**, *47*, 8582–8594.
63. Review: Wang, Y. J.; Hosta-Rigau, L.; Lomas, H.; Caruso, F. Nanostructured Polymer Assemblies Formed at Interfaces: Applications from Immobilization and Encapsulation to Stimuli-Responsive Release. *Phys. Chem. Chem. Phys.* **2011**, *13*, 4782–4801.
64. Semisotnov, G. V.; Rodionova, N. A.; Razzulyaev, O. I.; Uversky, V. N.; Gripas, A. F.; Gilmanshin, R. I. Study of the Molten Globule Intermediate State in Protein Folding by a Hydrophobic Fluorescent-Probe. *Biopolymers* **1991**, *31*, 119–128.
65. Nomura, Y.; Ikeda, M.; Yamaguchi, N.; Aoyama, Y.; Akiyoshi, K. Protein Refolding Assisted by Self-Assembled Nanogels as Novel Artificial Molecular Chaperone. *FEBS Lett.* **2003**, *553*, 271–276.
66. Nomura, Y.; Sasaki, Y.; Takagi, M.; Narita, T.; Aoyama, Y.; Akiyoshi, K. Thermoresponsive Controlled Association of Protein with a Dynamic Nanogel of Hydrophobized Polysaccharide and Cyclodextrin: Heat Shock Protein-Like Activity of Artificial Molecular Chaperone. *Biomacromolecules* **2005**, *6*, 447–452.
67. Krishnamurthy, V. M.; Kaufman, G. K.; Urbach, A. R.; Gitlin, I.; Gudiksen, K. L.; Weibel, D. B.; Whitesides, G. M. Carbonic Anhydrase as a Model for Biophysical and Physical-Organic Studies of Proteins and Protein-Ligand Binding. *Chem. Rev.* **2008**, *108*, 946–1051.
68. Wiegand, G.; Kukla, D.; Scholze, H.; Jones, T. A.; Huber, R. Crystal Structure Analysis of the Tetragonal Crystal Form and Preliminary Molecular Model of Pig-Heart Citrate Synthase. *Eur. J. Biochem.* **1979**, *93*, 41–50.
69. Pocker, Y.; Stone, J. T. The Catalytic Versatility of Erythrocyte Carbonic Anhydrase. III. Kinetic Studies of the Enzyme-Catalyzed Hydrolysis of p-Nitrophenyl Acetate. *Biochemistry* **1967**, *6*, 668–678.
70. Srere, P. A. Citrate Synthase. *Method Enzymol.* **1969**, *13*, 3–11.